High-Spatial-Resolution Fast BOTDA for Dynamic Strain Measurement Based on Differential Double-Pulse and Second-Order Sideband of Modulation

Yongkang Dong, Member, IEEE
Dexin Ba
Taofei Jiang
Dengwang Zhou
Hongying Zhang
Chengyu Zhu
Zhiwei Lu
Hui Li
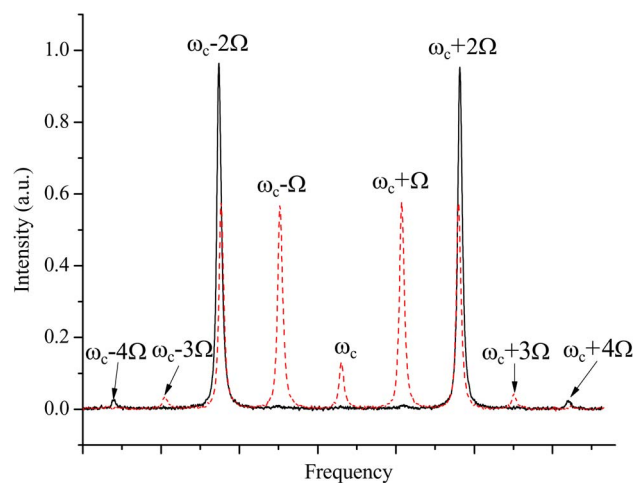Liang Chen
Xiaoyi Bao, Senior Member, IEEE

High-Spatial-Resolution Fast BOTDA for Dynamic Strain Measurement Based on Differential Double-Pulse and Second-Order Sideband of Modulation

Yongkang Dong,[1] *Member, IEEE,* **Dexin Ba,**[1] **Taofei Jiang,**[1] **Dengwang Zhou,**[1] **Hongying Zhang,**[2] **Chengyu Zhu,**[1] **Zhiwei Lu,**[1] **Hui Li,**[3] **Liang Chen,**[4] **and Xiaoyi Bao,**[4] *Senior Member, IEEE*

[1]Institute of Opto-Electronics, Harbin Institute of Technology, Harbin 150001, China
[2]Department of Optics Information Science and Technology, Harbin University of Science and Technology, Harbin 150001, China
[3]School of Civil Engineering, Harbin Institute of Technology, Harbin 150001, China
[4]Fiber Optics Lab, Department of Physics, University of Ottawa, Ottawa, ON K1N 6N5, Canada

Abstract: We demonstrate a high-spatial-resolution fast Brillouin optical time-domain analysis (BOTDA) for distributed dynamic strain measurement based on differential double-pulse and second-order sideband of modulation. The frequency-agility probe wave is obtained from the second-order sideband of the modulated light by using the microwave signal from a wideband arbitrary waveform generator (AWG), which reduces the bandwidth requirement of the AWG by half to ∼5.5 GHz. The differential double-pulse scheme is proposed to improve the spatial resolution while keeping the capability of dynamic measurement. In experiment, a spatial resolution of 20 cm is achieved by using a 52/50 ns differential double-pulse, and the distributed vibration measurement is demonstrated over a 50-m Panda polarization-maintaining fiber observing the vibration frequency of up to 50 Hz. With only five averages, the standard deviation of the strain accuracy is measured to be 14 $\mu\varepsilon$.

Index Terms: Brillouin optical time-domain analysis (BOTDA), dynamic measurement, strain measurement, high spatial resolution.

1. Introduction

Brillouin scattering based distributed optical fiber sensors have attracted considerable attentions in the past a few decades due to their capabilities of measuring temperature and strain over the sensing fibers [1]–[6]. The scheme of Brillouin optical time-domain analysis (BOTDA) is much preferable due to its high signal-to-noise ratio (SNR) and high accuracy. Usually, BOTDA includes two counter-propagating lights, i.e., a pump pulse and a CW probe wave, and the Brillouin gain spectra (BGS) of the sensing fibers can be obtained through scanning the frequency offset between the pump and the probe waves in the vicinity of the Brillouin frequency shift (BFS). Generally, there are two types of method to generate two frequency-stabilized lights for BOTDA, i.e., modulation with a microwave source [2] and frequency locking of two lasers [7], [8]. However, the optical frequency switching requires a finite time, so neither of them can realize fast frequency scanning, and thus, conventional BOTDA is usually regarded as only suitable for relative static measurement. Recently,

based on Brillouin optical correlation domain analysis (BOCDA), the distributed dynamic strain measurement of 1.3 Hz fiber vibration with a spatial resolution of 80 cm over 100-m fiber has been realized [9]. The slope assisted BOTDA was ever proposed for dynamic strain measurement, in which the frequency offset between the pump and the probe waves is set at the slope of the BGS, and the BFS change can be measured as the intensity variation of the probe wave [10], [11]. However, the measurement range is limited by the linear region of the BGS slope. More recently, a technique based on generation of frequency-agility microwave signal by an electric arbitrary waveform generator (AWG) was proposed to realize fast BOTDA or F-BOTDA, where the fast-changing of the signal frequency is achieved by pre-writing the desired frequencies into the memory of the AWG [12]. This method features a fast measurement time and a broad measurement range. With 13-ns pump pulses, a spatial resolution of 1.3 m was realized over a 100-m fiber observing a vibration frequency of up to 100 Hz [12].

The F-BOTDA faces the same problem as that in conventional BOTDA in terms of spatial resolution, which is limited to $\sim$1 m by the 10-ns phonon lifetime in silica fibers. Differential pulse-width pair (DPP) technique has ever been proposed to improve the spatial resolution of conventional BOTDA [13], based on which centimeter-order spatial resolution can be realized [14]. With DPP technique, two separate measurements are implemented by using two long pump pulses with different pulse-widths, and the differential signal is obtained by making subtraction between the two Brillouin signals, in which the spatial resolution can be improved by shorting the pulse-width difference. However, since the time interval between the two separate measurements is relatively long, it is not suitable for a dynamic measurement.

In this paper, we propose a modified DPP scheme, i.e., differential double-pulse, for a high-spatial-resolution F-BOTDA. Instead of using a single pump pulse in a usual case, two long pulses with different pulse-widths are used to form a differential double-pulse using as pump pulses, so that the two Brillouin signals are obtained almost at the same time, which allows for fast acquisition of the differential signal for the high-spatial-resolution F-BOTDA. In addition, we propose to use the second-order sideband as the probe wave through appropriately adjusting the operation point of the modulator with the carrier and odd-order sidebands being suppressed, and subsequently reducing the bandwidth requirement of the AWG by half to $\sim$5.5 GHz.

2. Measurement Scheme and Experimental Setup

2.1. Generation of Probe Wave Based on Second-Order Sideband of Modulation

In [12], for an F-BOTDA, the first-order lower sideband of the modulation was used as the probe wave through applying a frequency-agility microwave signal on an electro-optic modulator by pre-writing the desired frequencies into the memory of the AWG. As stated in [12], it is very difficult to find an available commercial AWG to output $\sim$11 GHz (BFS in silica fibers) microwave signal, and an I/Q microwave modulator was used to lift the output of a 500-MHz AWG to $\sim$11 GHz. In this paper, we propose to use the second-order sideband to reduce the bandwidth requirement of the AWG through appropriately adjusting the operation point of the modulator with the carrier and odd-order sidebands being suppressed.

A commonly used external intensity modulator is made by planar waveguide circuits designed in Mach–Zehnder interferometer (MZI) configuration. In this configuration, the input optical signal is equally split into two interferometer arms and then recombined. If the phase delays of the two MZI arms are ϕ_1 and ϕ_2, respectively, the combined output optical field E_o is

$$E_o(t) = \frac{1}{2} E_i e^{j\omega_c t} \cdot \left(e^{j\phi_1} + e^{j\phi_2} \right) \qquad (1)$$

where E_i is the complex amplitude of the input optical field, and ω_c is the carrier angular frequency. For a balanced MZI modulator, both arms have the same amount of the phase modulation $\pi/2 \cdot V_m/V_\pi \cos(\Omega t)$ but with opposite signs $\phi_1 = \phi_{10} + \pi/2 \cdot V_m/V_\pi \cos(\Omega t)$ and $\phi_2 = \phi_{10} - \pi/2 \cdot V_m/V_\pi \cos(\Omega t)$, where V_m and Ω are the amplitude and the angular frequency of the modulating
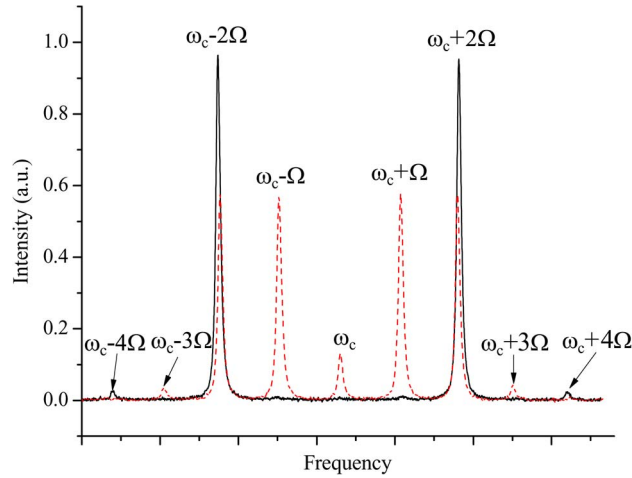
Fig. 1. Measured optical spectra of the modulated light. The solid curve shows the second-order sidebands dominating the spectrum when the modulator operates at the maximum transmission point and $\gamma = 2.405$; the dashed curve shows a complex spectrum with more frequencies when the modulator operates deviating from the optimal condition.

electrical signal, respectively, and V_π is the half-wave voltage of the modulator. The initial phase difference between the two MZI arms is $\phi_0 = \phi_{10} - \phi_{20}$, which determines the operation point of the modulator and can be controlled by adjusting the bias voltage.

When $\phi_0 = (2m + 1)\pi$, the modulator operates at the minimum transmission point, where the two first-order sidebands are generated and the carrier is suppressed. It is the well-known approach to generate the probe wave (using first-order lower sideband) for a BOTDA scheme, where the modulation frequency should be in the vicinity of BFS ~ 11 GHz [2]. When $\phi_0 = 2m\pi$, the modulator operates at the maximum transmission point, and (1) can be rewritten as

$$E_o(t) = E_i e^{j\omega_c t} \cdot \cos(\gamma \cos(\Omega t)) \qquad (2)$$

where $\gamma = \pi/2 \cdot V_m/V_\pi$. Equation (2) can also be expressed as

$$E_o(t) = E_i e^{j\omega_c t} \cdot \left[J_0(\gamma) + \sum_{n=1}^{\infty} (-1)^n J_{2n}(\gamma) \cdot (e^{j2n\Omega t} + e^{-j2n\Omega t}) \right]$$

$$= E_i \cdot \left\{ J_0(\gamma) e^{j\omega_c t} - J_2(\gamma) \cdot \left[e^{j(\omega_c + 2\Omega)t} + e^{j(\omega_c - 2\Omega)t} \right] + higher\ order\ terms \right\}. \qquad (3)$$

Here, $J_{2n}(\gamma)$ is Bessel function of the first kind. We note that, under this condition, the odd-order sidebands vanish; in the case of $\gamma = 2.405$, the optical term at carrier frequency also vanishes and the terms at $\omega_c \pm 2\Omega$ dominate the output. Although, now, there are higher order terms existing in the spectrum, their intensities can also be neglected for small γ. Fig. 1 shows the optical spectra of the modulated light measured by a scanning Fabry–Perot interferometer. When the modulator operates at the maximum transmission point and $\gamma = 2.405$, it (solid curve) shows that the second-order sidebands dominates the spectrum with other frequencies being suppressed; when the modulator operates deviating from the optimal condition, the optical terms at carrier frequency and odd-order sidebands appear (dashed curve). So through setting the modulator at the optimal condition, the second-order lower sideband can be filtered as the probe wave in a BOTDA system by using a narrowband filter, and subsequently the bandwidth requirement of the AWG is reduced by half to ~ 5.5 GHz.

2.2. Measurement Scheme

The conventional DPP technique includes two separate measurements using two pump pulses with different pulse-widths [13], [14]. It usually takes a relative long time to complete two separate
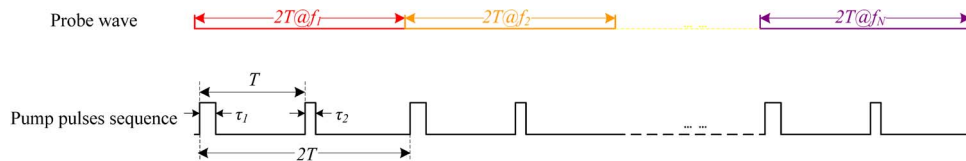
Fig. 2. Scheme of the probe wave and the pump pulses sequence for a high-spatial-resolution F-BOTDA. The frequency of probe wave is scanned from f_1 to f_N, and for each frequency its duration is $2T$. The pump pulses sequence includes many pairs of differential double-pulse, where the interval between the them also equals $2T$.
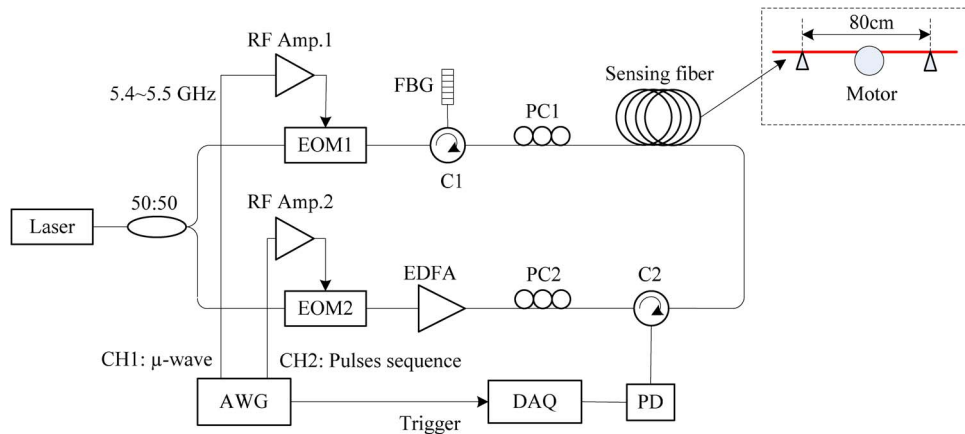

Fig. 3. Experimental setup. FBG: fiber Bragg grating, PC: polarization controller, C: circulator, PD: photo-detector, EOM: electro-optic modulator, DAQ: data-acquisition. An 80-cm section of fiber is vibrated periodically by an eccentric installed plastic ring driven by a motor.

measurements to obtain the differential signal, so that the conventional DPP technique is not suitable for improving the spatial resolution of F-BOTDA. To address this issue, we propose a modified DPP scheme, i.e., differential double-pulse, for a high-spatial-resolution F-BOTDA. As shown in Fig. 2, the differential double-pulse is composed of two long pulses with pulse-width of τ_1 and τ_2, where the interval T between the two pulses should be larger than the roundtrip time, i.e., the time taken for the light to make a round trip along the sensing fiber. As such, the two long pump pulses interact with the probe wave one after another, so that the differential Brillouin signals can be obtained almost at the same time, which allows for fast acquisition of the differential signal for the high-spatial-resolution F-BOTDA. The pump pulses sequence includes many pairs of differential double-pulse, where the interval between them equals to $2T$ and the number N equals to the frequency number of the probe wave. Using frequency-agility technique based on AWG, the frequency of probe wave is scanned from f_1 to f_N, and for each frequency, its duration is $2T$. The probe wave and the pump pulses sequence are synchronized and launched from the two ends of the sensing fiber to make sure that individual differential double-pulse interacts with one frequency of the probe wave.

2.3. Experimental Setup

The experimental setup is shown in Fig. 3. A narrow linewidth ~2 kHz fiber laser is used as the light source, which delivers an output power of 120 mW at around 1550 nm. A 3-dB coupler is used to split the output light into two parts providing the pump and the probe waves, respectively. The AWG is AWG7122C from Tektronix, which generates a frequency range of up to 9.6 GHz with the frequency switching time being as fast as 104 ps. The channel 1 of AWG7122C outputs frequency-agility microwave signal to modulate the light through an electro-optic modulator (EOM1), and the
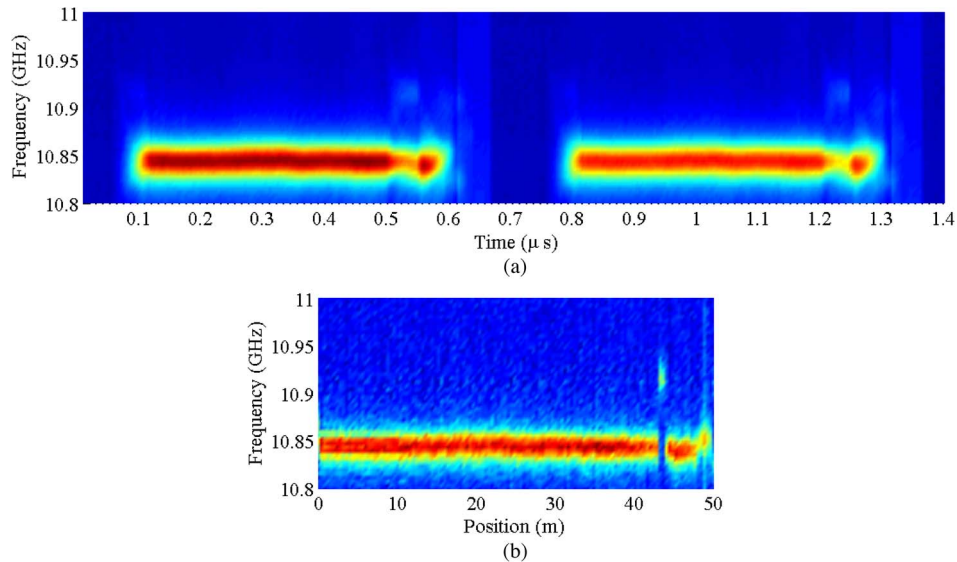
Fig. 4. Measured 3-D BGS of the sensing fiber (a) with 52/50 ns differential double-pulse and (b) after differential process. An 80-cm section of fiber located at the position of ~44 m was stretched.

second-order lower sideband is chosen as the probe wave by a narrow bandwidth fiber Bragg grating; the channel 2 is programmed to output electric pulses with the rise/fall time of 45 ps to generate pump pulses sequence through EOM2. The power of the probe wave is 50 μW, and the power of the pump pulses is amplified by an erbium-doped fiber amplifier (EDFA) to 600 mW. The signals from the two channels are amplified by two RF amplifiers to the suitable levels, and the delay between them can be programed and is intrinsically stable since they are from the same equipment. AWG7122C works in the burst mode, so that the sampling rate of the BGS measurement of the sensing fiber can be adjusted conveniently.

Polarization fading is a common issue for a BOTDA system using a standard single-mode fiber, and it can be removed by polarization scrambling and averaging a number of signals, which subsequently will slow down the effective sampling rate. A 50-m Panda polarization-maintaining fiber, whose BFS is 10.845 GHz at room temperature, is used as the sensing fiber to remove the polarization fading and improve the effective sampling rate. Two polarization controllers are used to ensure that the pump and probe waves are launched into the same principal axis of the sensing fiber. The frequency of the microwave signal from the AWG is scanned from 5.4 to 5.5 GHz with a step of 2 MHz, so that the frequency of the probe wave is down-shifted from 10.8 to 11 GHz with a step of 4 MHz and the frequency number $N = 51$. For each frequency, the duration of the probe wave is 1.4 μs, which is larger than the twice of the roundtrip time of the 50-m sensing fiber, i.e., 1 μs, so the total duration of the probe wave is 71.4 μs and the corresponding potential maximum sampling rate is as high as ~14 kHz. For pump pulses sequence, the differential double-pulse includes two long pulses, i.e., $\tau_1 = 52$ ns and $\tau_2 = 50$ ns, and their interval is 0.7 μs. To match with the probe wave, the pump pulses sequence contains 51 pair of differential double-pulse. The 2-ns pulse-width difference gives a spatial resolution of 20 cm in differential signal. The sampling rate of the DAQ is $f_{sampling} = 1.25$ GHz/s, corresponding to 8 cm/point.

3. Results and Discussions

An 80-cm section of fiber located at the position of ~44 m was first applied a static stress for test. The original measured data are a time trace of duration 71.4 μs. An average number of 5 was used to improve the SNR. The data process involves the following two steps: firstly, the time trace signal is divided into short segments of length $N_{seg} = 2T \cdot f_{sampling} (= 1750)$ forming a 51 × 1750 array, which includes the measured BGS with 52/50 ns differential double-pulse as shown in Fig. 4(a);
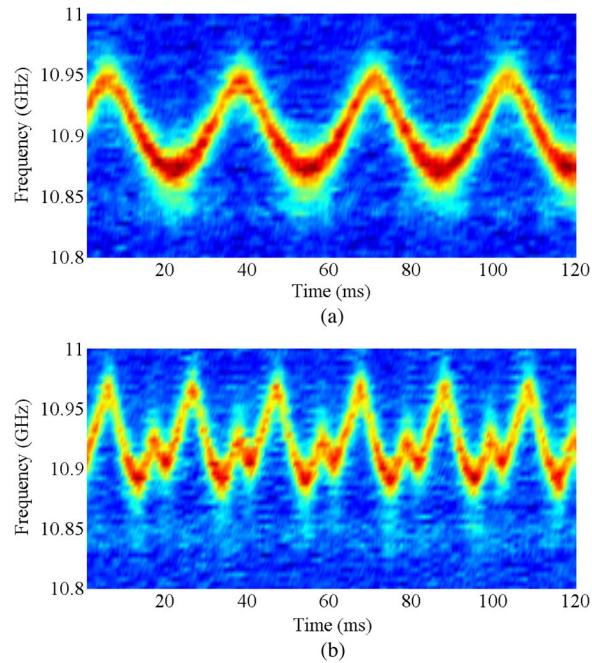
Fig. 5. Evolution of the measured BGS of the vibrated section of fiber at different vibration frequencies of (a) 33.3 Hz and (b) 50 Hz.
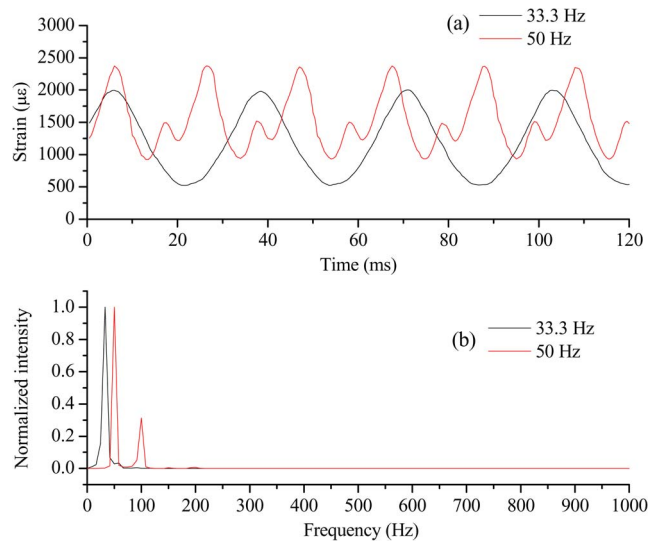

Fig. 6. (a) Measured dynamic strain as a function of time and (b) their power spectra at vibration frequencies of 33.3 and 50 Hz.

then, the 51 × 1750 array is divided from the middle into two 51 × 875 sub-arrays, and the differential signal is obtained by making subtraction between the two sub-arrays forming a new array as shown in Fig. 4(b). By comparison of Fig. 4(a) and (b), it is clear that the spatial resolution is considerably improved in differential signal in Fig. 4(b), in which the stretched 80-cm section of fiber is clearly shown with a 20-cm spatial resolution defined by the 2-ns pulse-width difference.

Then, we performed a dynamic strain measurement by applying vibration on the 80-cm section through an eccentric installed plastic ring driven by a motor. The interval between two adjacent

probe waves was set at 500 μs corresponding to a 2-kHz sampling rate of the measured BGS. A moving average of order 5 was used to improve the SNR, and thus, the effective sampling rate was reduced to 400 Hz. Fig. 5 shows the evolution of the measured BGS of the vibrated section of fiber at different vibration frequencies, i.e., Fig. 5(a) is for 33.3 Hz and Fig. 5(b) is for 50 Hz. The measured dynamic strain as a function of time is plotted in Fig. 6(a), and their power spectra are obtained by using Fourier transform, as shown in Fig. 6(b). We also observed a non-sine signal of the strain variation, which should be caused by the non-uniform vibration of the plastic ring, and the fundamental frequency of 50 Hz and the second-order harmonic of 100 Hz are clearly shown in Fig. 6(b). The standard deviation of the BFS is measured to be 0.7 MHz, corresponding to a strain accuracy of 14 $\mu\varepsilon$.

4. Conclusion

In this paper, we have demonstrated a high-spatial-resolution distributed dynamic strain measurement by using F-BOTDA. The second-order sideband has been proposed to provide the probe wave to reduce the bandwidth requirement of the AWG by half to ∼5.5 GHz, and a modified DPP scheme, i.e., differential double-pulse, has been proposed to improve spatial resolution for a dynamic measurement. The vibration frequency of up to 50 Hz has been observed over a 50-m Panda fiber with a spatial resolution of 20 cm by using 52/50 ns differential double-pulse. Since the potential effective maximum sampling rate can reach to ∼3 kHz with five averages, the vibration frequency of up to a few hundreds of Hz would be readily obtained.

References

[1] T. Horiguchi, K. Shimizu, T. Kurashima, M. Tateda, and Y. Koyamada, "Development of a distributed sensing technique using Brillouin scattering," *J. Lightwave Technol.*, vol. 13, no. 7, pp. 1296–1302, Jul. 1995.

[2] M. Nikles, L. Thevenaz, and P. A. Robert, "Simple distributed fiber sensor based on Brillouin gain spectrum analysis," *Opt. Lett.*, vol. 21, no. 10, pp. 758–760, May 1996.

[3] S. M. Maughan, H. H. Kee, and T. P. Newson, "57-km Single-ended spontaneous Brillouin-based distributed fiber temperature sensor using microwave coherent detection," *Opt. Lett.*, vol. 26, no. 6, pp. 331–333, Mar. 2001.

[4] X. H. Jia, Y. J. Rao, L. Chang, C. Zhang, and Z. L. Ran, "Enhanced sensing performance in long distance Brillouin optical time-domain analyzer based on Raman amplification: Theoretical and experimental investigation," *J. Lightwave Technol.*, vol. 28, no. 11, pp. 1624–1630, Jun. 2010.

[5] H. Liang, W. Li, N. Linze, L. Chen, and X. Bao, "High-resolution DPP-BOTDA over 50 km LEAF using return-to-zero coded pulses," *Opt. Lett.*, vol. 35, no. 10, pp. 1503–1505, May 2010.

[6] X. Bao and L. Chen, "Recent progress in optical fiber sensors based on Brillouin scattering at University of Ottawa," *Photon. Sens.*, vol. 1, no. 2, pp. 102–117, Jun. 2011.

[7] Y. Li, X. Bao, F. Ravet, and E. Ponomarev, "Distributed Brillouin sensor system based on offset locking of two distributed feedback lasers," *Appl. Opt.*, vol. 47, no. 2, pp. 99–102, Jan. 2008.

[8] L. Thevenaz, S. Le Floch, D. Alasia, and J. Troger, "Novel schemes for optical signal generation using laser injection locking with application to Brillouin sensing," *Meas. Sci. Technol.*, vol. 15, no. 8, pp. 1519–1524, Aug. 2004.

[9] K. Y. Song, M. Kishi, Z. He, and K. Hotate, "High-repetition-rate distributed Brillouin sensor based on optical correlation-domain analysis with differential frequency modulation," *Opt. Lett.*, vol. 36, no. 11, pp. 2062–2064, Jun. 2011.

[10] R. Bernini, A. Minardo, and L. Zeni, "Dynamic strain measurement in optical fibers by stimulated Brillouin scattering," *Opt. Lett.*, vol. 34, no. 17, pp. 2613–2615, Sep. 2009.

[11] Y. Peled, A. Motil, L. Yaron, and M. Tur, "Slope-assisted fast distributed sensing in optical fibers with arbitrary Brillouin profile," *Opt. Exp.*, vol. 19, no. 21, pp. 19 845–19 854, Oct. 2011.

[12] Y. Peled, A. Motil, and M. Tur, "Fast Brillouin optical time domain analysis for dynamic sensing," *Opt. Exp.*, vol. 20, no. 8, pp. 8584–8591, Apr. 2012.

[13] W. Li, X. Bao, Y. Li, and L. Chen, "Differential pulse-width pair BOTDA for high spatial resolution sensing," *Opt. Exp.*, vol. 16, no. 26, pp. 21 616–21 625, Dec. 2008.

[14] Y. Dong, H. Zhang, L. Chen, and X. Bao, "2-cm-Spatial-resolution and 2-km-range Brillouin optical fiber sensor using a transient differential pulse pair," *Appl. Opt.*, vol. 51, no. 9, pp. 1229–1235, Mar. 2012.